Application of Machine Learning to Signal Detection in Underwater Wireless Optical Communication Links

Mohamed Nennouche, Mohammad Ali Khalighi, Alexis Dowhuszko, Djamal Merad

Application of Machine Learning to Signal Detection in Underwater Wireless Optical Communication Links

1st Mohamed Nennouche
Aix-Marseille University, CNRS
Centrale Med, LIS
Marseille, France
Mohamed.Nennouche@lis-lab.fr

2nd Mohammad Ali Khalighi
Aix-Marseille University, CNRS
Centrale Med, Fresnel Institute
Marseille, France
Ali.Khalighi@fresnel.fr

3rd Alexis Dowhuszko
Dept. Information & Commun. Eng.
Aalto University
02150 Espoo, Finland
alexis.dowhuszko@aalto.fi

4th Djamal Merad
Aix-Marseille University, CNRS
University of Toulon, LIS
Marseille, France
Djamal.Merad@lis-lab.fr

5th Jean-Marc Boï
Aix-Marseille University, CNRS
University of Toulon, LIS
Marseille, France
Jean-Marc.Boi@lis-lab.fr

***Abstract*—We consider the application of a machine-learning (ML)-based method to the demodulation of the received signal in underwater wireless optical communication (UWOC) links. This approach is justified when the underwater optical channel is subject to strong variations due to various phenomena such as pointing errors and turbulences, which directly impact the received optical power, requiring accurate and agile channel estimation. The investigated ML method is based on the well-known K-nearest neighbors (KNN). We demonstrate excellent link performance for different types of modulation schemes even under high data rates and low received optical powers, for instance, achieving effective bit rates of 2.96 and 2.54 Gbps using 16-QAM and 32-QAM modulation schemes, respectively, at a received optical power of -16.4 dBm. We also discuss the implementation aspects of the proposed approach, including its computational complexity.**

***Index Terms*—Underwater wireless optical communications; Machine learning; Signal demodulation; KNN classification.**

I. Introduction

With the expansion of human activities underwater and the recent advancements in the Internet of Underwater things (IoUT), encompassing robotics and underwater sensors and vehicles, underwater wireless optical communications (UWOC) has been receiving a surge of interest in recent years due to its capability to provide exceptionally high data rates and energy-efficient transmission over short to moderate link ranges [1]–[3]. Despite the significant potential of the UWOC technology, its performance is hindered by various factors due to the unique characteristics of the underwater channel. These factors include: water absorption and scattering, especially notable in relatively high-turbidity waters; pointing errors, in particular, when communicating with a mobile unit or a floating node at the water surface; and, in specific situations, air bubbles, fish schools, and oceanic turbulence [4]–[10].

To effectively tackle the challenges posed by channel impairments in complex and unpredictable underwater scenarios, it is crucial to employ efficient signal transmission methods ensuring resilient communication links between the involved underwater nodes. Specifically, accurately estimating the channel state information under extreme variability conditions and for high-speed links can be challenging and requires substantial resource allocation for pilot transmission. Under such conditions, leveraging machine learning (ML) techniques for signal demodulation shows great potential. ML's capacity to "learn" from training data and extract "information" makes it a compelling solution. It has demonstrated impressive results across various domains, including signal processing and wireless communications [11].

Several recent works have explored the use of ML-based or deep-learning (DL)-based methods for signal detection in UWOC systems. For instance, Jiang *et al.* in [12] proposed a two-connection multilayer perceptron network (MLP), in which the first subnetwork functions as a channel equalizer and the second one as a demodulator. This was applied to a UWOC link using DC-biased optical orthogonal frequency-division multiplexing (DCO-OFDM) modulation and a single-photon avalanche diode (SPAD) at the receiver, showing results superior to conventional signal detection in terms of bit-error rate (BER). Also, Ma *et al.* in [13] proposed an UWOC demodulator based on three-layer deep belief networks (DBNs) and evaluated its performance with a real signal dataset (the same that we use in this work), showing that it outperforms maximum likelihood classification (MLC), convolutional neural networks (CNNs), and the naive Bayes-based classifier (NBC) in terms of effective bit rate (EBR) for different considered modulation techniques and received signal levels. Lastly, the authors of [14] proposed a deep neural network (DNN)-based

This work was partly supported by the French PACA (Provence, Alpes, Côte d'Azur) Regional Council and the École Centrale Méditerranée, Marseille, France. It was also based upon work from COST Action CA19111 (European Network on Future Generation Optical Wireless Communication Technologies, NEWFOCUS), supported by COST (European Cooperation in Science and Technology).

on-off keying (OOK) demodulator and compared its BER performance with an optimal-threshold [15] OOK demodulator at different signal-to-noise ratios (SNRs), without needing any prior knowledge of the channel.

This paper studies the use of ML for signal demodulation in an UWOC system. We consider different intensity-based signal modulation techniques, including OOK, pulse position modulation (PPM), quadrature amplitude modulation (QAM) with sub-carrier intensity modulation (SIM) [1], and DCO-OFDM [16]. The considered ML algorithm is the K-nearest neighbors (KNN) [17], which is a high-performance algorithm for classifying data samples, with proven efficiency in RF signal detection [18]. We demonstrate the exceptional performance of KNN in terms of classification accuracy and EBR, even at relatively low received signal levels. Considering the lower complexity of the proposed approach, particularly in contrast to that of [13], and its robustness across different modulation schemes, it emerges as a highly promising solution for signal detection within the studied context.

The remainder of the paper is organized as follows: Section II provides a brief overview of the system model. Then, Section III introduces the KNN-based UWOC demodulator along with the experimental dataset utilized for training and performance evaluation. The numerical results demonstrating the performance of the proposed approach for UWOC signal demodulation are presented and discussed in Section IV. Finally, Section V concludes the paper.

II. System Model

We have used in our study the data set made available by Ma *et al.* related to the work presented in [13]. This dataset was obtained by an experimental set-up, where at the transmitter a blue laser diode was used with a maximum output optical power of 20 mW, and at the receiver a plano-convex lens was used before an avalanche photo-diode (APD). The received signal was resampled with a sampling rate of 12.5 Giga-samples/s (Gsps). The optical signal propagated through a controlled underwater channel in a water tank with a total length of 21 m with the use of a metal optical filter with variable neural density to simulate the attenuation of light in water and thus obtain the different levels of received optical power (ROP), as shown in the synaptic diagram of Fig. 1 (the dataset can be accessed via the link provided in [19], see [13]).

We have selected six modulation schemes from the original dataset, i.e., OOK, 4-PPM, 4-QAM, 8-QAM, 16-QAM, 32-QAM, with three different numbers M of sample points per symbol, i.e., $M = 8$, 16, and 64 (QAM schemes are based on SIM). In addition, we consider the DCO-OFDM modulation scheme with 4 (main) subcarriers, an IFFT size of 10, and 4-QAM constellation mapping. The ROP in the experiments was varied from -30 to -10 dBm [13]. The transmitted symbol $x(t)$ is then expressed as:

$$x(t) = \mathrm{Re}\left[s(t)\, p(t)\, e^{j2\pi f_c t}\right] \ , \quad 0 \le t \le T \tag{1}$$

where $s(t)$, $p(t)$, f_c, and T represent the baseband symbol, pulse shaping function (considered here as rectangular, for simplicity), sub-carrier frequency (for QAM schemes), and symbol duration, respectively, and $\mathrm{Re}[.]$ denotes the real part.

The signal detection task can be analogized to the classification of received symbols. This way, the algorithm performance (in other words, the classification quality) is evaluated based on the two metrics of *accuracy* [17] and EBR [1], defined as:

$$\text{Accuracy } = \frac{\text{number of correctly classified symbols}}{\text{total number of samples}}, \tag{2}$$

$$\text{EBR } = \text{Accuracy } B\,\frac{F_s}{M}, \tag{3}$$

where B, F_s, and M refer to the number of bits per symbol, sampling frequency, and number of samples per symbol, respectively.

III. KNN-based signal demodulation

KNN is one of the simplest supervised ML algorithms, first developed by E. Fix and J. Hodges in 1951 [20]. Like any other supervised ML algorithm, KNN requires two phases: a learning phase, followed by an evaluation phase. The learning phase consists of putting each training dataset sample in a space where each dimension represents one of the dataset *features*. In our case, features are the different samples of a symbol, where the symbol itself represents the *class* (or label). During the evaluation phase, a new set of symbols is introduced into the space, and the distance of each symbol from its K nearest neighbors is calculated based on a distance metric. The most commonly used distances are Euclidean, Manhattan, and Canberra [21]. By selecting the K nearest neighbors, the classes (symbols) to which they belong are observed, and the new received symbol is assigned the majority class in its neighborhood. This operation is conducted across all received symbols, and the algorithm's performance is assessed by comparing predicted classes to the actual classes of each received symbol. Subsequently, the overall performance is evaluated based on classification accuracy. The two most key parameters in the KNN algorithm are the selected distance metric and the number of nearest neighbors K considered for classification.

Figure 2 illustrates an example of the application of KNN to a two-dimensional classification scenario, where the Euclidean distance is considered as metric. First, we place the training samples, which are partitioned into two categories, represented by blue and brown squares. Then, for a new test sample, shown by a yellow triangle, we should determine its class; for $K = 3$, the majority class is blue, whereas for $K = 7$, the majority class is brown. This indicates the importance of careful selection of the K parameter. In our case, after investigating the appropriate distance metric and number of neighbors, achieving a balanced compromise between algorithm complexity and performance, we have selected the Euclidean distance d, defined below, and set the number of neighbors to $K = 7$.

$$d(a,b) = \sqrt{\sum_{0}^{M}(x_i - y_i)^2} \tag{4}$$

Remember that M denotes the number of samples per symbol. Also, x_i represents the i^{th} sample of the new element x added to the feature space, and y_i denotes the i^{th} sample of a training symbol y.

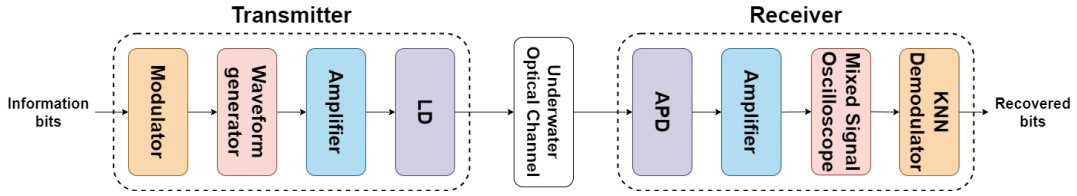

Fig. 1: Schematic diagram of the experimental setup, similar to the approach used in [13].

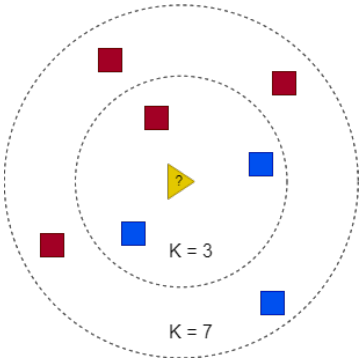

Fig. 2: Illustration of KNN based on the Euclidean distance metric with $K = 3$ and 7.

IV. Numerical results and discussions

To evaluate the algorithm performance, we have carried out training and algorithm evaluation for each modulation scheme separately, where 70% of the dataset for each ROP level was used for model training (i.e., 70000, 35000, and 8750 samples for $M = 8$, 16, and 64, respectively), and the remainder for performance evaluation.

We have compared in Fig. 3 the algorithm performance in terms of accuracy versus ROP in the evaluation phase, for the considered modulation schemes, $M = 8$, 16, and 64, and an ROP range from -28 to -16 dBm. Note that the considered ROP range corresponds to the available dataset. Also, the performance in the training phase is similar to the evaluation phase, and are not presented for the sake of brevity.

As expected, the performance generally improves with an increase in the ROP, since symbols can be better distinguished and classified. We can also see from these results that the parameter M plays a predominant role in the classification quality: As seen from Fig. 3a, with $M = 8$ and for 4-PPM, 8-QAM, 16-QAM, and 32-QAM, we obtain an accuracy of less than 35%. Note, we conjecture that the better performance of 16-QAM, compared to 8-QAM, is due to the limited quality of the available dataset. Only for OOK and 4-QAM we can reach an accuracy of more than 50%.

Furthermore, we notice from Fig. 3b that by increasing M to 16, for most modulation schemes, the training quality and the performance improve, exceeding 60% accuracy. The performance even reaches 100% for OOK and 4-QAM for ROP> -22.5 dBm. This trend is confirmed in Fig. 3c with $M = 64$, where we observe a significant performance of the model performance, attaining perfect classification for OOK, 4-PPM, and 4-QAM for ROP> -25 dBm, for instance.
The significant impact of the parameter M can in particular be seen in the case of 4-PPM. For this modulation, the performance is rather poor with $M = 8$ and 16, whereas a significant performance improvement is achieved with $M = 64$, surpassing even 4-QAM. Overall, these results demonstrate the outstanding performance of the proposed algorithm for signal detection and its ability of accurate classification for a wide range of modulation schemes.

We have further presented in Fig. 4 the EBR plots for $M = 8$, 16, or 64 samples per symbol, considering the sampling rate of 12.5 Gsps. These results highlight the trade-off between the classification performance and the parameter M that needs to be considered. For a too small M (here, $M = 8$, shown in Fig 4a), the algorithm struggles in accurately classifying the different symbols of a modulation scheme, especially, for higher-order modulations. Note that in Fig. 4a, the superior performance of 4-QAM over OOK can be explained by the relationship between the accuracy and EBR, see (3), resulting in a better ratio of Accuracy/EBR for the former scheme. We notice that the best results are obtained for $M = 16$, see Fig. 4b, where, for instance, EBRs of about 3 and 1.5 Gbps are obtained for 16-QAM and 4-QAM, respectively, for sufficiently high ROPs. On the other hand, although for $M = 64$ from Fig. 4c the best accuracy is achieved, given that this represents 4 times as more samples as for $M = 16$, the EBR remains below 1 Gbps (which is still noticeable, however), see (3). Overall, from these results, we can deduce that a trade-off needs to be made between the classification accuracy and the number of samples per symbol to reach the target EBR.

To make a comparison with the DBN approach proposed in [13], we have contrasted the classification accuracy of the two methods in Fig. 5 for 16-QAM modulation and $M = 32$. We notice that our proposed approach performs very similarly to DBN, but with the added benefit of lower computational complexity, making it more suitable for practical implementation.

Lastly, Fig. 6 shows the performance in terms of accuracy and EBR for the case of DCO-OFDM signaling with 4-QAM modulation, and an ROP range between -23.5 and -13 dBm. We notice that, like for the previously-considered modulation schemes, the accuracy increases with increased ROP, as the algorithm can better recognize the received symbols. For ROP> -19 dBm, we obtain an accuracy close to 100%, which is equivalent to an EBR of 10 Gbps. We also obtain a good EBR performance of higher than 1 Gbps for lower ROPs. We have also shown on this figure the results corresponding to the DBN method from [13, Fig. 5], where we notice a similar performance. Once again, our KNN-based approach maintains an advantage due to its lower computational complexity.

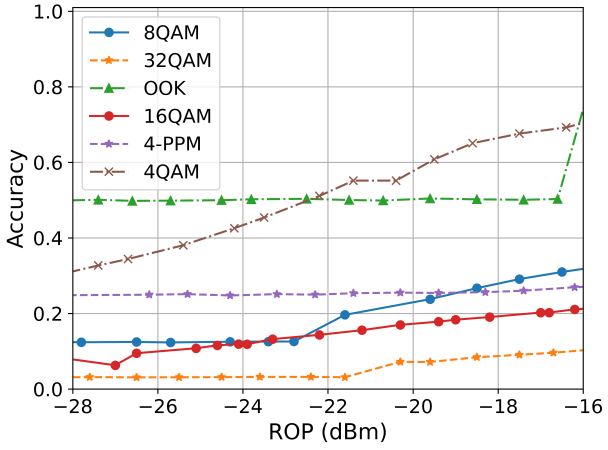

(a)

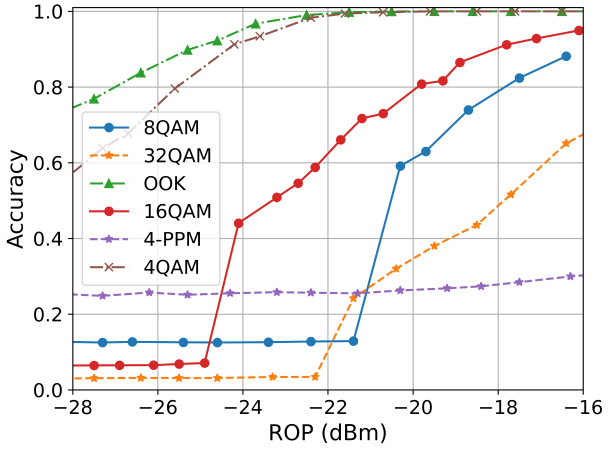

(b)

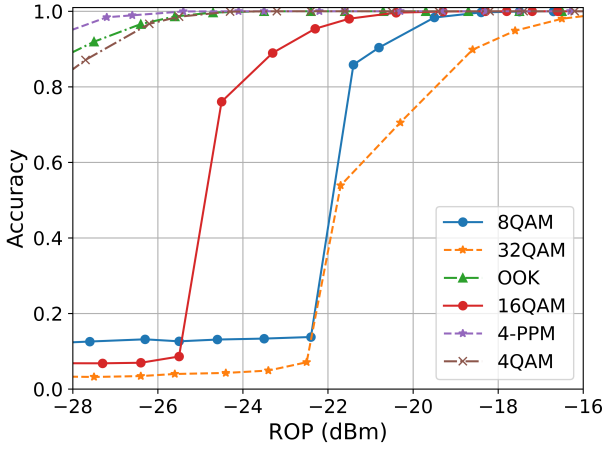

(c)

Fig. 3: Percentage of the correctly detected symbols using the KNN-based demodulator for different modulation schemes; (a) $M = 8$, (b) $M = 16$, (c) $M = 64$ samples per symbol.

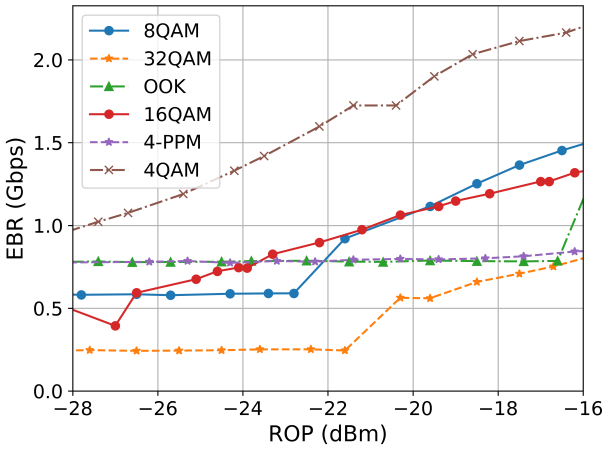

(a)

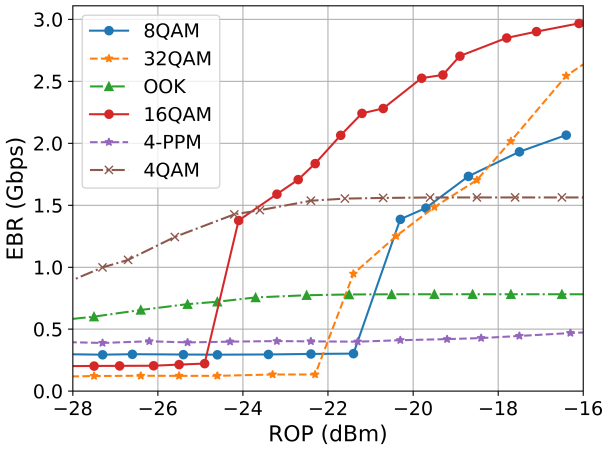

(b)

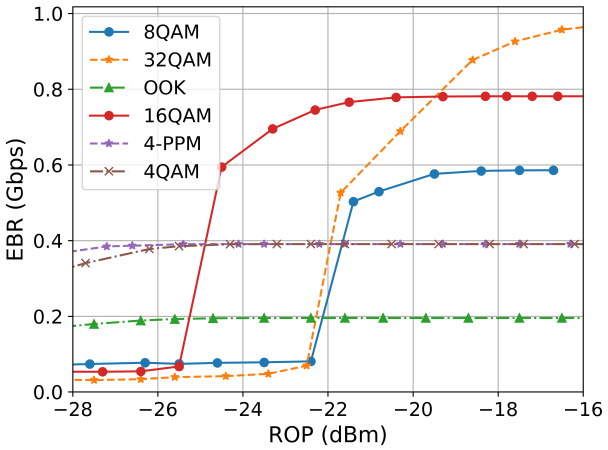

(c)

Fig. 4: Achieved EBR using the KNN-based demodulator for (a) $M = 8$, (b) $M = 16$, and (c) $M = 64$.

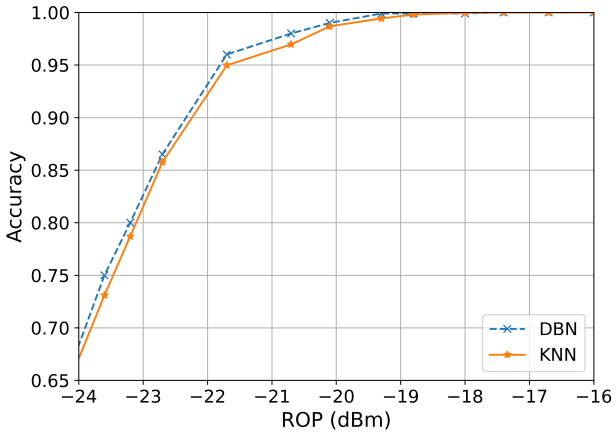

Fig. 5: Accuracy of the proposed KNN-based demodulator for 16-QAM modulation and $M = 32$, compared with that of the DBN approach, presented in [13].

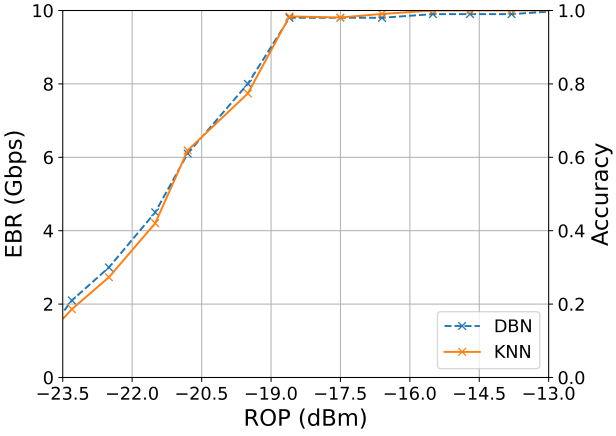

Fig. 6: EBR and accuracy of the KNN-based demodulator for DCO-OFDM signaling with 4-QAM modulation per sub-carrier and FFT size of 10, compared with that of the DBN approach in [13].

V. Conclusions and Discussions

In this work, we investigated the efficiency of KNN-based signal demodulation in the context of UWOC. We demonstrated the significant performance of the proposed method in terms of both accuracy and EBR by considering various modulation schemes and signal sampling rates. It is worth mentioning that the computational complexity of the proposed method remains very low, where we only need to calculate the distance between each new received symbol and the symbols making up the training base, and then to select the K-nearest neighbors.

Nevertheless, the limitation of the proposed approach is the inability of the model to "learn" below a certain ROP level, which is around -25 dBm, where consequently, the classification is not effective. This is mainly because at very low ROPs, the noise level is too high, making it impossible to distinguish between different symbols. This problem can be addressed in different ways, which is the subject of our future research. One potential research direction is to develop more robust and efficient models, such as those based on MLPs or CNNs, which could provide better performance at lower ROPs.

References

[1] Z. Zeng, S. Fu, H. Zhang, Y. Dong, and J. Cheng, "A survey of underwater optical wireless communications," *IEEE Commun. Surveys Tuts.*, vol. 19, no. 1, pp. 204–238, 2016.

[2] M. A. Khalighi, C. J. Gabriel, L. M. Pessoa, and B. Silva, *Visible Light Communications: Theory and Applications*. CRC-Press, 2017, ch. Underwater Visible Light Communications, Channel Modeling and System Design, pp. 337–372.

[3] M. Jahanbakht, W. Xiang, L. Hanzo, and M. R. Azghadi, "Internet of underwater things and big marine data analytics: a comprehensive survey," *IEEE Commun. Surveys Tuts.*, vol. 23, no. 2, pp. 904–956, 2021.

[4] B. Cochenour, L. Mullen, and J. Muth, "Temporal response of the underwater optical channel for high-bandwidth wireless laser communications," *IEEE J. Ocean. Eng.*, vol. 38, no. 4, pp. 730–742, Oct. 2013.

[5] C. Gabriel, M. A. Khalighi, S. Bourennane, P. Léon, and V. Rigaud, "Monte-Carlo-based channel characterization for underwater optical communication systems," *IEEE J. Opt. Commun. Netw.*, vol. 5, no. 1, pp. 1–12, Jan. 2013.

[6] M. V. Jamali, A. Mirani, A. Parsay, B. Abolhassani, P. Nabavi, A. Chizari, P. Khorramshahi, S. Abdollahramezani, and J. A. Salehi, "Statistical studies of fading in underwater wireless optical channels in the presence of air bubble, temperature, and salinity random variations," *IEEE Trans. Commun.*, vol. 66, no. 10, pp. 4706–4723, Oct. 2018.

[7] E. Zedini, H. M. Oubei, A. Kammoun, M. Hamdi, B. S. Ooi, and M.-S. Alouini, "Unified statistical channel model for turbulence-induced fading in underwater wireless optical communication systems," *IEEE Trans. Commun.*, vol. 67, no. 4, pp. 2893–2907, Apr. 2019.

[8] M. Elamassie and M. Uysal, "Vertical underwater visible light communication links: Channel modeling and performance analysis," *IEEE Trans. Commun.*, vol. 19, no. 10, pp. 6948–6959, Oct. 2020.

[9] A. S. Ghazy, S. Hranilovic, and M. A. Khalighi, "Angular MIMO for underwater wireless optical communications: Link modelling and tracking," *IEEE J. Ocean. Eng.*, vol. 46, no. 4, pp. 1391–1407, 2021.

[10] I. C. Ijeh, M. A. Khalighi, M. Elamassie, S. Hranilovic, and M. Uysal, "Outage probability analysis of a vertical underwater wireless optical link subject to oceanic turbulence and pointing errors," *IEEE J. Opt. Commun. Netw.*, vol. 14, no. 6, pp. 439–453, 2022.

[11] H. Dahrouj, R. Alghamdi, H. Alwazani, S. Bahanshal, A. A. Ahmad, A. Faisal, R. Shalabi, R. Alhadrami, A. Subasi, M. T. Al-Nory *et al.*, "An overview of machine learning-based techniques for solving optimization problems in communications and signal processing," *IEEE Access*, vol. 9, pp. 74 908–74 938, May 2021.

[12] R. Jiang, C. Sun, L. Zhang, X. Tang, H. Wang, and A. Zhang, "Deep learning aided signal detection for SPAD-based underwater optical wireless communications," *IEEE Access*, vol. 8, pp. 20 363–20 374, Jan. 2020.

[13] S. Ma, Z. Zhang, H. Li, J. Xu, H. Zhang, S. Zhang, and S. Li, "Design of DBN based demodulator in underwater wireless optical communications," in *2020 IEEE/CIC Int. Conf. Commun. in China (ICCC Workshops)*. IEEE, Sep. 2020, pp. 179–184.

[14] O. N. Mohammed Salim, S. A. Adnan, and A. H. Mutlag, "Underwater optical wireless communication system performance improvement using convolutional neural networks," *AIP Advances*, vol. 13, no. 4, 2023.

[15] M. T. Dabiri, S. M. S. Sadough, and M. A. Khalighi, "FSO channel estimation for OOK modulation with APD receiver over atmospheric turbulence and pointing errors," *Optics Commun.*, vol. 402, pp. 577–584, Apr. 2017.

[16] T. Essalih, M. A. Khalighi, S. Hranilovic, and H. Akhouayri, "Optical OFDM for SiPM-based underwater optical wireless communication links," *Sensors*, vol. 20, no. 21, p. 6057, Oct. 2020.

[17] F.-L. Luo, *Machine Learning for Future Wireless Communications*. Wiley-IEEE Press, 2020.

[18] M. W. Aslam, Z. Zhu, and A. K. Nandi, "Automatic modulation classification using combination of genetic programming and KNN," *IEEE Trans. Wireless Commun.*, vol. 11, no. 8, pp. 2742–2750, June 2012.

[19] Original Dataset from [13] , https://pan.baidu.com/s/1SwjP78KZXyd6aF7TuUmuQQ, last accessed May 2024.

[20] E. Fix and J. L. Hodges, "Discriminatory analysis, nonparametric discrimination," 1951, Technical Report 4, USAF School of Aviation Medicine.

[21] R. Ehsani and F. Drabløs, "Robust distance measures for KNN classification of cancer data," *Cancer Informatics*, vol. 19, p. 1176935120965542, Oct. 2020.